How to cite: *Angew. Chem. Int. Ed.* **2022,** *61,* e202207963
International Edition: doi.org/10.1002/anie.202207963
German Edition: doi.org/10.1002/ange.202207963

Superacids

Calix[4]pyrrolato Stibenium: Lewis Superacidity by Antimony(III)-Antimony(V) Electromerism

Marcel Schorpp[+]*, Ravi Yadav*[+]*, Daniel Roth, and Lutz Greb**

Abstract: Lewis superacids enable the activation of highly inert substrates. However, the permanent presence of a Lewis superacidic center comes along with a constantly increased intolerance toward functional groups or ambient conditions. Herein, we describe a strategy to unleash Lewis superacidity by electromerism. Experimental and computational results indicate that coordinating a Lewis base to Δ-calix[4]pyrrolato-antimony(III) triggers a ligand redox-noninnocent coupled transfer into antimony(V)-state that exhibits Lewis superacidic features. Lewis acidity by electromerism establishes a concept of potential generality for powerful yet robust reagents and on-site substrate activation approaches.

Lewis acids play vital roles from the forefront of chemical research to industrial applications.[1] An increasing affinity of a Lewis acid usually correlates with higher reactivity and facilitates transformations of exceedingly inert substrates.[2] Lewis acids with a fluoride ion affinity (FIA) larger than SbF_5 have been classified as Lewis superacids (LSA).[3] Many compounds with central elements spanning the periodic table have been developed.[2] While the fierce reactivity of a LSA is generally promising, it usually comes at the expense of intolerance for functional groups or ambient conditions. This can cause the formation of side products or premature quenching, effectively hampering broad applicability. A compound that shows LSA properties only after being triggered by external stimuli would be a valuable improvement. Group 15 Lewis acids have gained particular attention in recent years.[4] By the introduction of strongly electron-withdrawing substituents or positive charge(s), several pnictonium-,[5] pnictocenium-ion[6] or pnictorane[7] Lewis acids have been obtained. Beyond these classical strategies to increase Lewis acidity, structural deformation emerged as an alternative concept.[8] We recently isolated anti-van't-Hoff-Le-Bel anionic calix-[4]pyrrolato aluminates and the isoelectronic neutral silicon-(IV) species.[9–11] Structural constraint-enforced square-planar coordination at the central element resulted in much higher Lewis acidity than in the corresponding tetrahedral counterparts.[9,12] In earlier work, Floriani and Nocera exploited the redox noninnocence of the calix[4]pyrrole ligand (Cx[4]) in complexes with transition metals.[13] A two-electron oxidation is accompanied by the dearomatization of two pyrrole moieties and the formation of a cyclopropane ring (so-called **Δ**-form, see Figure 1a). For instance, when $[Fe^{III}Cx[4]^{Me}]^-$ was treated with 3 equiv of ferrocenium, $[Fe^{II}\Delta\Delta Cx[4]^{Me}]$ formed as the product of fourfold oxidation of the ligand-backbone with simultaneous reduction of the central Fe^{III} to Fe^{II} (see Figure 1b).[14] This redox-induced electron transfer (RIET)[15] illustrates the intimate communication between the ligand scaffold and the central element, allowing for electromerism (i.e., valence tautomerism), that is, the change of electronic distribution by external stimuli.[16]

Electromerism is typically associated with transition metal complexes of redox-active ligands, whereas examples with main-group elements are scarce.[18] The germanium-(II)porphyrin represents a seminal case for a p-block element (Figure 1c).[17] Dissolution of the deep green $Ge^{II}TPP$ in pyridine results in the bright-red bis-pyridine adduct of germanium(IV) with a two-electron reduced, antiaromatic porphyrin backbone. Changed oxidation states of main-group elements are associated with stark reactivity variation. We surmised that combining the Cx[4] ligand's redox noninnocence with redox-flexible group 15 elements might enable switching between low-affinity Pn^{III} and high-affinity Pn^{V} states (Figure 1d). The following study establishes the coordination chemistry of the "$[Cx[4]^{Et}]^{4-}$" and oxidized "$[\Delta Cx[4]^{Et}]^{2-}$" ligand towards antimony. It illustrates the concept of Lewis superacidity triggered by electromerism and ligand redox-noninnocence.

The reaction of deprotonated $Cx[4]^{Et}$-salts with $SbCl_5$ (a strong oxidant) resulted in a product mixture with concomitant formation of paramagnetic species. Hence, a synthesis employing Sb^{III} precursors was pursued. By the reaction of fully deprotonated $Li_4Cx[4]^{Et}\cdot 3THF$ and one equivalent of $SbCl_3$ in THF at −78 °C, $[Li(THF)_3][SbCx[4]^{Et}]$ **Li^{THF}-1** was formed and isolated on a multi-gram scale in 76 % yield

[*] Dr. M. Schorpp,[+] Dr. R. Yadav,[+] D. Roth
Anorganisch-Chemisches Institut, Ruprecht-Karls-Universität Heidelberg
Im Neuenheimer Feld 270, 69120 Heidelberg (Germany)
Prof. Dr. L. Greb
Department of Chemistry and Biochemistry—Inorganic Chemistry, Freie Universität Berlin
Fabeckstr. 34/36, 14195 Berlin (Germany)
E-mail: lutz.greb@fu-berlin.de
[+] These authors contributed equally to this work.

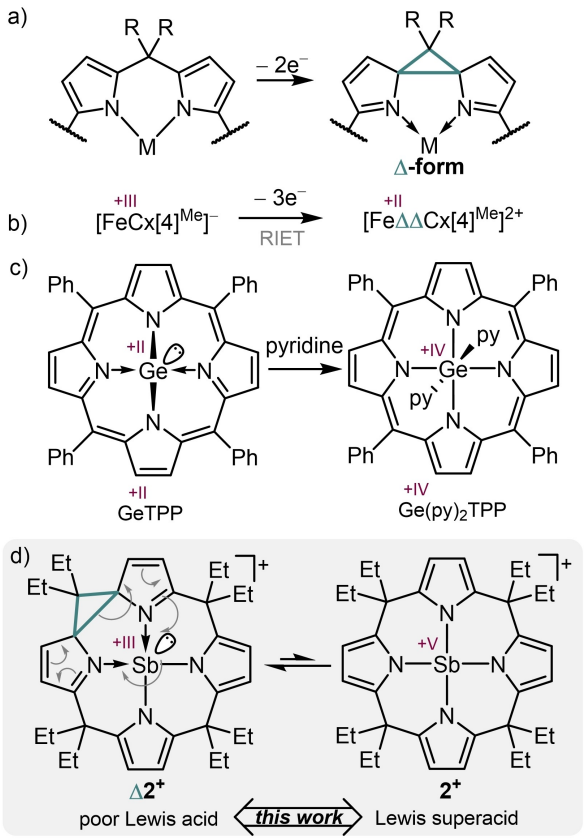

Figure 1. a) Two-electron oxidation of the bispyrrol subunit in $Cx[4]^{R}$ ligand to the Δ-form. b) Three electron oxidation of $[Fe^{III}Cx[4]^{Me}]^{-}$ and RIET in the formation of $[Fe^{II}\Delta\Delta Cx[4]^{Me}]^{2+}$.[14] c) Redox isomerism in a germanium tetraphenylporphyrin complex by addition of pyridine.[17] d) Proposed ligand-element electromerism of $[Sb^{III}\Delta Cx[4]^{Et}]^{+}$ **Δ2⁺** and $[Sb^{V}Cx[4]^{Et}]^{+}$ **2⁺**.

(Figure 2a). Single crystals suitable for scXRD analysis were obtained by layering a solution of **Li^{THF}-1** in THF with n-hexane (molecular structure see Supporting Information).[27] A better structural model was obtained from $[PPh_4][SbCx[4]^{Et}]$ **PPh_4-1** generated by salt metathesis between **Li^{THF}-1** and PPh_4Cl in dichloromethane (Figure 2b).

The rigid $Cx[4]^{Et}$ ligand scaffold enforces a rare non-VSEPR square-pyramidal coordination at Sb,[19] which lies at 0.862(1) Å distance above the N_4 plane. The interatomic distances between Sb and pyrrolato-N are almost identical ($d_{N\text{-}Sb}$(avg.) = 2.160(18) Å; ($d_{N\text{-}Sb}$(range) = 2.1340(18)–2.1821(17) Å) and are in between structurally related neutral corrolato-Sb^{III} ($d_{N\text{-}Sb}$(avg.) = 2.121(3) Å[20]) and cationic pthalocyaninato-Sb^{III} ($d_{N\text{-}Sb}$(avg.) = 2.227(3)[21]). In contrast to the tetrahedral to square planar deformation in Cx(4)-Al^{III} and Si^{IV},[9,10] the VSEPR-conform pseudo-trigonal bipyramidal to square-pyramidal deformation has only minimal effects on the FMO energies (slight destabilization of both HOMO (ΔE = 0.18 eV) and LUMO (ΔE = 0.34 eV) in comparison to the computed VSEPR-conform $[Sb(pyrrolato)_4]^{-}$). It is noteworthy that the lone pair at Sb is energetically buried (HOMO-4), in line with the observed reactivity of **Li^{THF}-1** towards $HNTf_2$, resulting in the protonation of the 2-position at a pyrrole moiety in the ligand backbone (see Supporting Information).

To generate cation **2⁺**, the antimonites **[cat.]-1** were reacted with a range of oxidizing agents (discussion see Supporting Information). Best results were obtained by treating **Li^{THF}-1** or **PPh_4-1** with ferrocenium salts [Fc][A] ($[A]^{-}$ = $[SbF_6]^{-}$, $[PF_6]^{-}$, Figure 3a). Precipitation yielded **2[A]** as orange solid in 70 % of varying purity (70–95 %) with leftover [Fc][A] as contaminant. Analytically pure samples of **2[A]** and single crystals suitable for scXRD analysis were obtained by layering of a concentrated DCM solution with n-hexane. The molecular structure (**Δ2[SbF_6]** Figure 3b, and **Δ2[PF_6]** see Supporting Information) revealed $[Sb^{III}\Delta Cx[4]^{Et}]^{+}$ with distorted square-pyramidal coordination ($d_{N4plane\text{-}Sb}$ = 0.945(1) Å) by two aromatic pyrrolato-moieties ($d_{N\text{-}Sb}$ = 2.0778(15) Å) and two dearomatized

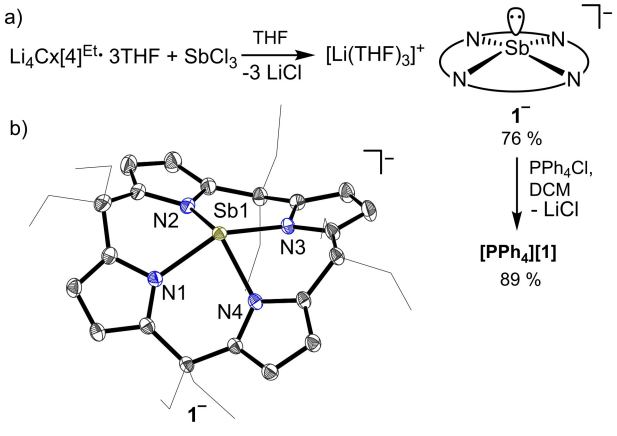

Figure 2. a) Protocol for the synthesis of **[Li^{THF}]-1** and **[PPh_4]-1**. b) Molecular structure of **[PPh_4]-1**. $[PPh_4]^{+}$, DCM, protons omitted and ethyl-groups drawn as wireframe for clarity. Thermal displacement ellipsoids drawn at 50% probability.

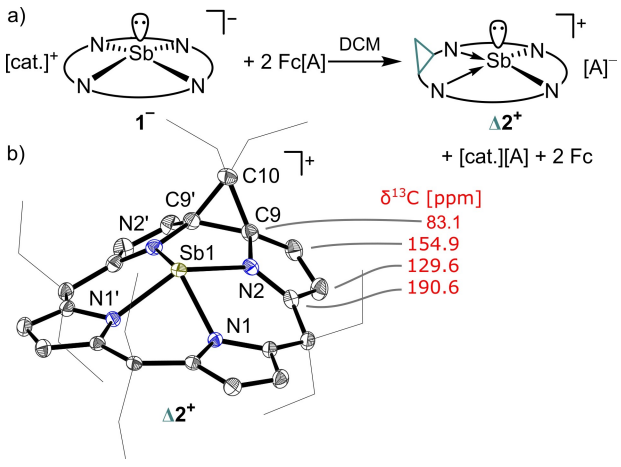

Figure 3. a) Protocol for the synthesis of **Δ2[A]**. b) Molecular structure of **Δ2[SbF_6]**. $[SbF_6]^{-}$ and protons omitted and ethyl-groups drawn as wire frame for clarity. Thermal displacement ellipsoids set at 50% probability.

pyrrole-moieties ($d_{N\text{-}Sb}$ = 2.2589(16) Å). This molecular structure is in line with obtained NMR data of **Δ2[A]** in solutions of CD_2Cl_2.

Hence, the presumed equilibrium between **Δ2$^+$** and **2$^+$** (Figure 1d) was found to lie on the side of Sb^{III} with the oxidized **Δ**-ligand. Indeed, computed thermodynamics (@DSD-BLYP(D3BJ)/def2-QZVPP, COSMO-RS DCM) revealed the Sb^{III}-form **Δ2$^+$** to be favored by $\Delta_R H^\circ_{gas(solv)}$ = 228.6(246.5) kJ mol^{-1} (Scheme 1a). The computed local minimum **2$^+$**, a square planar anti-van't-Hoff-Le-Bell Sb^V, appears thermally inaccessible. Indeed, the **Δ2$^+$** cation was found experimentally stable against $[SbF_6]^-$ (FIA(SbF_5) = 496), $[PF_6]^-$ (FIA(PF_5) = 384) and even $[BF_4]^-$ (FIA(BF_3) = 346),[22] thus proving the Lewis acidity of **Δ2$^+$** to be as evidently little (cf. Scheme 1b and later discussion). Yet, when **Δ2[SbF$_6$]** was dissolved in THF-d_8 for NMR analysis, spontaneous polymerization of the solvent was observed. We assumed that the coordination of a Lewis base (LB; here THF) at Sb^{III} induces a transformation to Sb^V by coupling with the ligand's redox noninnocence (cf. Figure 1d). Accordingly, reacting **Δ2[SbF$_6$]** with an excess of pyridine in CD_2Cl_2 showed rapid consumption of the starting material by NMR analysis. The obtained reaction mixture was left for crystallization, providing single crystals of the pyridine adduct of SbF_5 (py-SbF_5). Hence, during the course of this reaction, abstraction of a fluoride ion from SbF_6^- had taken place, which conforms to the requirement to classify a compound as a Lewis superacid.[2] The reaction was repeated analogously with **Δ2[PF$_6$]**. ^{19}F- and ^{31}P NMR gave spectroscopic evidence for the anion decomposition with the formation of the respective adduct py-PF_5. In both cases, ^{1}H NMR spectra of the reaction revealed a mixture of at least two Cx[4]^{Et}-containing species. Most importantly, the disappearance of ^{13}C-chemical shifts for dearomatized pyrroles in all observed species indicated the reduction of ΔCx[4]^{Et} to non-ΔCx[4]^{Et} forms. ^{1}H NOESY NMR experiments verified proximity between the flanking ethyl groups to a pyridine moiety. ^{19}F NMR spectra contained a broadened singlet resonance at $\delta(^{19}F) = -112.7$ with cross-peaks in ^{1}H–^{19}F(HMBC) NMR spectra one of the new Cx[4]^{Et} species. Similar ^{19}F NMR shifts ($\delta(^{19}F) = -105.4$) had been observed for Sb-bound fluorides at hexacoordinated corrole Sb^V complex.[23] The separation of this product mixture was impossible due to instability, and no structural proof could be obtained by scXRD. However, ESI and LIFDI-mass spectrometry confirmed products of composition **2-py-F** and **2-py$^+$**. Reacting **Δ2[PF$_6$]** with neutral Lewis bases (e.g. 3,5-lutidine or PMe_3) resulted in similar anion degradation as in the case of added pyridine (see section 2.7 in the Supporting Information). *Hence, these results indicated the formation of a Lewis superacid upon activating with a Lewis-base.*

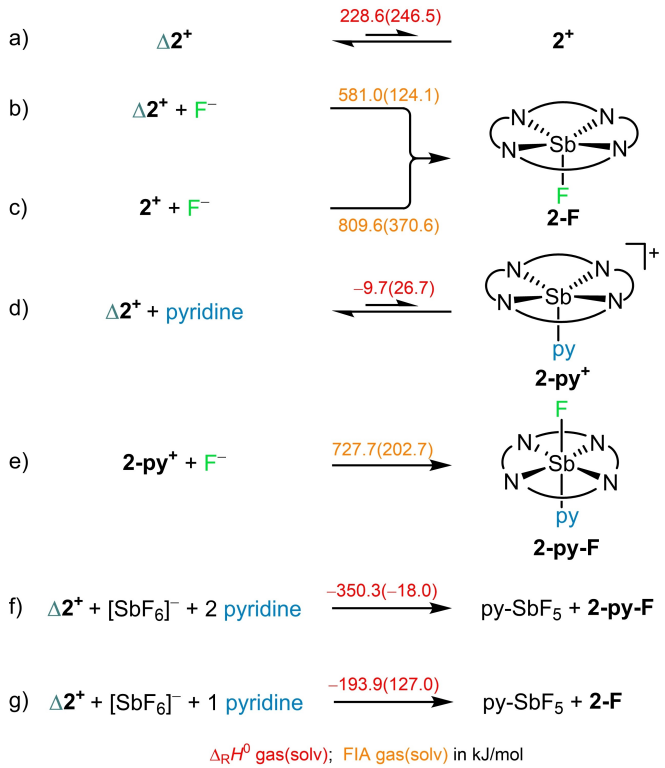

Scheme 1. Computed gas-phase and solvated thermodynamics for a) spontaneous and d) triggered) Sb^{III} to Sb^V transformation. b), c) and e) FIA for **Δ2$^+$**, **2$^+$** and **2-py$^+$**. f), g) Computed gas-phase and solvated thermodynamics for the $[SbF_6]^-$ decomposition. DSD-BLYP(D3BJ)/def2-QZVPP (COSMO-RS, DCM)/PBEh-3c.

The plausibility and rationale of this process was elucidated by DFT-computations. Adduct formation between **Δ2$^+$** and pyridine to Sb-bound **2-py$^+$** is mildly exothermic (Scheme 1d), with a very shallow transition state of $\Delta H^{\ddagger} = +11.5$ kJ mol^{-1} (Supporting Information). The lone pair from Sb^{III} (**Δ2$^+$**) shifts into the ligand (**2-py$^+$**) and creates a Sb^V species with a FIA significantly increased by 145 kJ mol^{-1} compared to **Δ2$^+$** (referenced to TMS^+/TMS-F anchor points @ DSD-BLYP(D3BJ)/def2-QZVPP COSMO-RS DCM, cf. Scheme 1b,e).[22,24] Remarkably, the FIA of the square-planar **2$^+$** is dampened by only 80 kJ mol^{-1} upon coordination of pyridine (cf Scheme 1c,e). Accordingly, the experimentally observed decomposition of $[SbF_6]^-$ is reproduced in silico when 2 equivalents of pyridine are employed (see Scheme 1f,g). In line with this finding, incomplete consumption of **Δ2$^+$** was observed when reacting **Δ2[PF$_6$]** with less than 2 equivalents of pyridine.

Further experiments and computations were performed to scrutinize this interpretation. The reaction between **Δ2$^+$[A]** and a stronger F^--source ($[NBu_4][Ph_3SiF_2]$) in the absence of pyridine lead to a C–F bound species which was assigned as the product of cyclopropyl ring-opening (cf. Supporting Information; $\delta(^{19}F) = -145.3$ (m) ppm). This latter adduct can be converted back to **Δ2$^+$** by reaction with $B(C_6F_5)_3$ (FIA = 448 kJ mol^{-1}).[22] Importantly, cyclopropyl ring-opening by pyridine attack at the quaternary carbon is unlikely due to a computed reaction barrier of 26 kJ mol^{-1} higher in enthalpy compared to the attack of pyridine at Sb^{III} (see section 4.1 in the Supporting Information). Hence, the Sb^{III} to Sb^V transformation appears to happen under kinetic control in the presence of specific Lewis bases. When a **Δ2$^+$** salt of a mixture of counteranions **[Al(OR^F)$_4$]** (OR^F = $OC(CF_3)_3$) and $LiPF_6$ was treated with DMAP, the formation of $[Sb\text{–}F(DMAP)_4]^{2+}$ was observed by scXRD (Scheme 2a). *This result supports the interaction of the Lewis base*

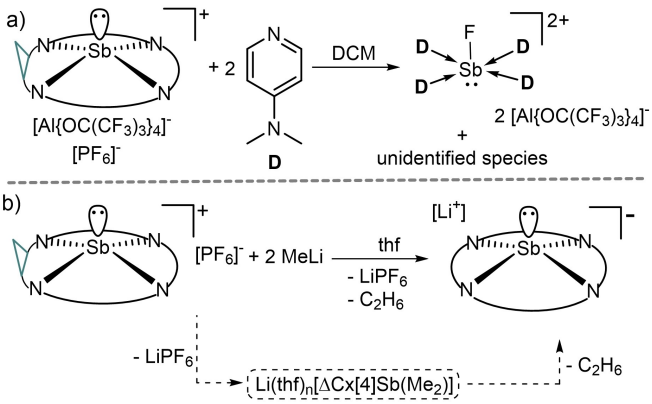

Scheme 2. Experimental indications for a) fluoride abstraction and Lewis base binding to antimony, and b) ligand reduction by MeLi attack and oxidative coupling to ethane.

with the antimony center and fluoride abstraction during the process.

Additional evidence for the proposed electromerism was obtained by reacting **Δ2[PF$_6$]** with two equivalents of MeLi. The clean and quantitative formation of **Li^{THF}-1** and $LiPF_6$, along with the formation of ethane gas, was observed by NMR spectroscopy (Scheme 2b). The di-methyl-Sb^V intermediate $[Li(thf)_n]Sb\text{-}Me_2Cx[4]^{Et}$] was detected by mass spectrometry, undergoing reductive elimination potentially in a bimolecular process. Importantly, subjecting **Li$_2$-(THF)ΔCx[4]^{Et}** (the **Δ**-ligand *without* an antimony center) to MeLi did not lead to the reduction of the ligand but an unselective attack in the ligand backbone (see section 2.8 in the Supporting Information). *This observation underscores the critical role of antimony as the primary binding site and redox modulator.*

Figure 4 depicts the FMO energies and LUMO shapes of the **2$^+$** local minimum, the **Δ2$^+$** global minimum, and the adduct **2-py$^+$**. Of the three considered species, the square planar **2$^+$** has the LUMO of lowest energy, p_z type at Sb^V.

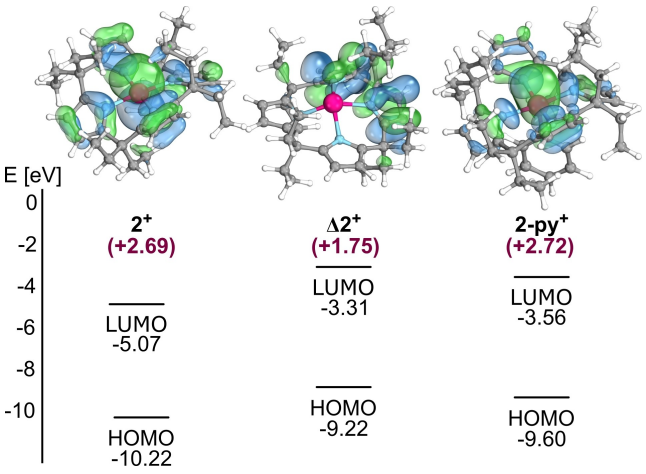

Figure 4. Frontier orbital energies and Kohn–Sham LUMOs in **2$^+$** vs **Δ2$^+$** and **2-py$^+$** (NBO charge at Sb in brackets).

Due to the unfavorably high energy of **2$^+$** (Scheme 1a), it does not play a role independently. However, its chemistry can be stimulated by the coordination of selected Lewis bases. Indeed, the energy of the LUMO in **2-py$^+$** drops below that of **Δ2$^+$** and maintains Sb-character. In other words, the LUMO of a compound (**Δ2$^+$**) is lowered upon adduct formation with a Lewis base (**2-py$^+$**)—to the best of our knowledge, an unprecedented finding (see reference[8c] for the computational prediction of a related effect). The σ-type ligand pyridine stabilizes the Sb^V-form while retaining p_z-character for Lewis acidic behavior at the opposite side for reactions with further substrates (such as SbF_6^-). Indeed, the computed NBO-charges at Sb change massively upon electromerism from +1.75 (**Δ2$^+$**) to +2.71 (**2-py$^+$**). Overall, these characteristics rationalize the uniqueness of the present observation.

In conclusion, we synthesized non-VSEPR antimonite(III)-anion **[cat.]-1** with square pyramidal coordination by a porphyrinogen ligand scaffold. Ligand-centered two-electron oxidation affords a tetracoordinate stibenium(III)-ion **Δ2$^+$** with stability towards $[MF_6]^-$ (M = Sb,P) and $[BF_4]^-$, illustrating its marginal Lewis acidity. By adding a sufficiently strong neutral Lewis-base, rapid decomposition of the employed counter ions occurs. DFT computations, spectroscopic observations, and control experiments indicate the formation of a transient stibonium(V)-ion with Lewis superacidic properties. Counterintuitively, Lewis base coordination does not lead to the saturation of the acceptor element, but induces a significant reactivity increase. One might be reminded of Lewis base binding induced electrophilicity enhancement operative in n-σ* Lewis base catalysis.[25] However, the electromerism suggested in the present case results in a substantially stronger electronic redistribution (ΔNBO-charge at antimony of +0.96) compared to the subtle, sometimes even inverted polarization changes found in Lewis base catalysis.[26] Although currently limited by competing decomposition channels of the intermediates, the concept of triggerable Lewis superacidity by electromerism will enable applications, such as on-site catalyst activation. Indeed, unexpected activity in a hydrodefluorination reaction preliminarily supports these hypotheses.

Acknowledgements

We thank Prof. H.-J. Himmel for his constant support. Financial support was provided through the European Research Council (ERC) under the European Union's Horizon 2020 research and innovation program (grant agreement No948708). The federal state of Baden-Württemberg is greatly acknowledged for providing computational resources at the BWFor/BWUni Cluster. Open Access funding enabled and organized by Projekt DEAL.

Conflict of Interest

The authors declare no conflict of interest.

Data Availability Statement

The data that support the findings of this study are available in the Supporting Information of this article.

Keywords: Antimony · Lewis Superacid · Ligand Redox Noninnocence · Main-Group · Structural Constraint

[1] a) A. Corma, H. García, *Chem. Rev.* **2003**, *103*, 4307; b) H. Yamamoto, K. Ishihara, *Acid catalysis in modern organic synthesis*, Wiley-VCH, Weinheim, **2008**; c) D. W. Stephan, G. Erker, *Angew. Chem. Int. Ed.* **2015**, *54*, 6400; *Angew. Chem.* **2015**, *127*, 6498; d) D. W. Stephan, *J. Am. Chem. Soc.* **2015**, *137*, 10018.

[2] L. Greb, *Chem. Eur. J.* **2018**, *24*, 17881.

[3] L. O. Müller, D. Himmel, J. Stauffer, G. Steinfeld, J. Slattery, G. Santiso-Quiñones, V. Brecht, I. Krossing, *Angew. Chem. Int. Ed.* **2008**, *47*, 7659; *Angew. Chem.* **2008**, *120*, 7772.

[4] J. M. Bayne, D. W. Stephan, *Chem. Soc. Rev.* **2016**, *45*, 765.

[5] a) C. B. Caputo, L. J. Hounjet, R. Dobrovetsky, D. W. Stephan, *Science* **2013**, *341*, 1374; b) S. Postle, V. Podgorny, D. W. Stephan, *Dalton Trans.* **2016**, *45*, 14651; c) D. Tofan, F. P. Gabbaï, *Chem. Sci.* **2016**, *7*, 6768; d) B. Pan, F. P. Gabbaï, *J. Am. Chem. Soc.* **2014**, *136*, 9564.

[6] a) J. Zhou, L. L. Liu, L. L. Cao, D. W. Stephan, *Chem* **2019**, *58*, 5407; b) P. Jutzi, T. Wippermann, C. Krüger, H.-J. Kraus, *Angew. Chem. Int. Ed. Engl.* **1983**, *22*, 250; *Angew. Chem.* **1983**, *95*, 244.

[7] K. M. Marczenko, C.-L. Johnson, S. S. Chitnis, *Chem. Eur. J.* **2019**, *25*, 8865.

[8] a) J. C. Gilhula, A. T. Radosevich, *Chem. Sci.* **2019**, *10*, 7177; b) M. Yang, D. Tofan, C.-H. Chen, K. M. Jack, F. P. Gabbaï, *Angew. Chem. Int. Ed.* **2018**, *57*, 13868; *Angew. Chem.* **2018**, *130*, 14064; c) K. M. Marczenko, S. Jee, S. S. Chitnis, *Organometallics* **2020**, *39*, 4287.

[9] F. Ebner, H. Wadepohl, L. Greb, *J. Am. Chem. Soc.* **2019**, *141*, 18009.

[10] F. Ebner, L. Greb, *Chem* **2021**, *7*, 2151–2159.

[11] F. Ebner, P. Mainik, L. Greb, *Chem. Eur. J.* **2021**, *27*, 5120.

[12] F. Ebner, L. Greb, *J. Am. Chem. Soc.* **2018**, *140*, 17409.

[13] a) J. Jubb, D. Jacoby, C. Floriani, A. Chiesi-Villa, C. Rizzoli, *Inorg. Chem.* **1992**, *31*, 1306; b) J. Jubb, C. Floriani, A. Chiesi-Villa, C. Rizzoli, *J. Am. Chem. Soc.* **1992**, *114*, 6571; c) L. Bonomo, E. Solari, R. Scopelliti, C. Floriani, N. Re, *J. Am. Chem. Soc.* **2000**, *122*, 5312; d) J. Bachmann, D. G. Nocera, *J. Am. Chem. Soc.* **2004**, *126*, 2829.

[14] J. Bachmann, D. G. Nocera, *J. Am. Chem. Soc.* **2005**, *127*, 4730.

[15] J. S. Miller, K. S. Min, *Angew. Chem. Int. Ed.* **2009**, *48*, 262; *Angew. Chem.* **2009**, *121*, 268.

[16] a) E. Evangelio, D. Ruiz-Molina, *C. R. Chim.* **2008**, *11*, 1137; b) T. Tezgerevska, K. G. Alley, C. Boskovic, *Coord. Chem. Rev.* **2014**, *268*, 23; c) R. M. Buchanan, C. G. Pierpont, *J. Am. Chem. Soc.* **1980**, *102*, 4951.

[17] J. A. Cissell, T. P. Vaid, G. P. A. Yap, *J. Am. Chem. Soc.* **2007**, *129*, 7841.

[18] a) S. Yao, A. Kostenko, Y. Xiong, C. Lorent, A. Ruzicka, M. Driess, *Angew. Chem. Int. Ed.* **2021**, *60*, 14864; *Angew. Chem.* **2021**, *133*, 14990; b) Y. Xiong, D. Chen, S. Yao, J. Zhu, A. Ruzicka, M. Driess, *J. Am. Chem. Soc.* **2021**, *143*, 6229; c) M. G. Chegerev, A. V. Piskunov, A. A. Starikova, S. P. Kubrin, G. K. Fukin, V. K. Cherkasov, G. A. Abakumov, *Eur. J. Inorg. Chem.* **2018**, 1087; d) M. G. Chegerev, A. A. Starikova, A. V. Piskunov, V. K. Cherkasov, *Eur. J. Inorg. Chem.* **2016**, 252; e) L. Greb, *Eur. J. Inorg. Chem.* **2022**, e202100871.

[19] C. M. Lemon, S. J. Hwang, A. G. Maher, D. C. Powers, D. G. Nocera, *Inorg. Chem.* **2018**, *57*, 5333.

[20] S. Mondal, A. Garai, P. K. Naik, J. K. Adha, S. Kar, *Inorg. Chim. Acta* **2020**, *501*, 119300.

[21] R. Kubiak, M. Razik, *Acta Crystallogr. Sect. C* **1998**, *54*, 483.

[22] P. Erdmann, J. Leitner, J. Schwarz, L. Greb, *ChemPhysChem* **2020**, *21*, 987.

[23] I. Luobeznova, M. Raizman, I. Goldberg, Z. Gross, *Inorg. Chem.* **2006**, *45*, 386.

[24] H. Böhrer, N. Trapp, D. Himmel, M. Schleep, I. Krossing, *Dalton Trans.* **2015**, *44*, 7489.

[25] S. E. Denmark, G. L. Beutner, *Angew. Chem. Int. Ed.* **2008**, *47*, 1560; *Angew. Chem.* **2008**, *120*, 1584.

[26] S. E. Denmark, G. L. Beutner in *Lewis Base Catalysis in Organic Synthesis* (Eds.: E. Vedejs, S. E. Denmark), Wiley-VCH, Weinheim, **2016**, pp. 31–54.

[27] Deposition Numbers 1240732, 2086686, 2108206, 2108300, 2108301, 2108302 and 2108303 contain the supplementary crystallographic data for this paper. These data are provided free of charge by the joint Cambridge Crystallographic Data Centre and Fachinformationszentrum Karlsruhe Access Structures service.

Manuscript received: May 30, 2022
Accepted manuscript online: August 4, 2022
Version of record online: August 25, 2022